ESTABLISHMENT OF DUCTILITY FACTOR BASED ON ENERGY ABSORPTION AND EVALUATION OF PRESENT METHODS

Franklin Y. Cheng, Kenneth B. Oster and Prasert Kitipitayangkul

SYNOPSIS

This paper reviews two conventional definitions of ductility factor on the basis of rotation and curvature and then proposes two new formulations based on the dissipated strain energy. The advantages and disadvantages of each of the methods are discussed along with some illustrations. These four ductility definitions are finally employed in the seismic response studies of a ten-story, one-bay plane rigid frame and a ten-story, one-bay three-dimensional building system with concrete floors and steel columns. The plane structure is subjected to two-dimensional ground motions and the responses of the three-dimensional building are due to the interacting earthquake motions of two horizontal and one vertical. The numerical examples reveal that the ductility definitions based on the energy are more suitable to interacting ground motions than the conventional definitions and that the interacting earthquake motions can demand larger ductilities than those for one dimensional motion.

RESUME

Cette communication fait état des définitions conventionnelles des facteurs de ductilité basés sur la rotation ou courbure. Deux autres nouvelles définitions sont aussi proposées mais basées sur le concept de l'énergie dissipée. Les avantages et désavantages de chaque définition sont présentés. Pour les quatre définitions de ductilité, deux bâtiments de dix étages sont étudiés dont l'un est traité comme un cadre planaire, l'autre comme une structure en trois dimensions. Les exemples numériques démontrent que la définition de la ductilité basée sur le concept énergétique est plus adéquate.

Franklin Y. Cheng, Professor of Civil Engineering at the University of Missouri-Rolla, received his Ph.D. from the University of Wisconsin-Madison in 1966.
Kenneth B. Oster is Assistant Professor of Civil Engineering and Engineering Mechanics at the Indiana Institute of Technology. As a former graduate student of Dr. F.Y. Cheng, he received his Ph.D. from the University of Missouri-Rolla in 1976.
Prasert Kitipitayangkul is a doctoral candidate in Civil Engineering Department, University of Missouri-Rolla.

INTRODUCTION

In seismic design, economic considerations generally require that some of the energy input into a structural system during strong earthquake motions be dissipated by large inelastic deformations. It is common to express the maximum required inelastic deformation in terms of ductility factor. However, there is not any uniform technique of measuring the ductility. The current methods of evaluating the ductility factor are only suitable for a limited type of hysteresis. In this paper four definitions of the ductility ratio for determining the ductility requirement of earthquake structures are included. The corresponding excursion ratio is also given to indicate the total plastic rotation or dissipated energy of each node of structural members during the loading process. These four ductility ratios are based on rotation of antisymmetric bending, curvature, variable energy, and mixed energy. Each of these methods will be reviewed and then some comparative studies of numerical results will be revealed.

DESCRIPTION OF METHODS

1. Ductility ratio based on rotation of antisymmetric bending-- The traditional definition (1, 2) of the ductility ratio μ_1 is based on anti-symmetrical bending of a structural member. The half cycle of the moment-rotation curve for either end of such a member is shown in Fig. 1 based on a bilinear material response. Both ends of the member become plastic when the end moment reaches the plastic moment, M_p. The ductility ratio based on anti-symmetrical bending is defined as the maximum absolute nodal rotation $|\theta|_{max}$ divided by the yield rotation θ_y. Using the notation of Fig. 1, μ_1 can be written as

$$\mu_1 = \frac{|\theta|_{max}}{\theta_y} = \frac{\theta_y + \alpha}{\theta_y} = 1 + \frac{\alpha}{\theta_y} \qquad (1)$$

where α = plastic rotation. Since the yield rotation is based on anti-symmetrical bending, it can be expressed as $\theta_y = M_p L/6EI$, where L is the length of the member and EI is the member's flexural rigidity.

The excursion ratio ε_1 corresponding to the ductility ratio can be defined as the total plastic rotation of a node of a member divided by the yield rotation of the joint. Thus

$$\varepsilon_1 = \sum_{i=1}^{N_u} \frac{\alpha_i}{\theta_y} \tag{2}$$

where N_u = total number of times the node becomes plastic, α_i = plastic rotation of the node during a half cycle of rotation i, and θ_y = yield rotation of anti-symmetric bending. In terms of the ductility ratios the excursion ratio can be written as

$$\varepsilon_1 = \sum_{i=1}^{N_u} (\mu_{1i} - 1) \tag{3}$$

where μ_{1i} is the ductility ratio for the half cycle plastic rotation i.

Discussion of the method--When considering a typical moment resisting frame subjected to both horizontal and vertical components of an earthquake, anti-symmetrical bending is seldom present in any of the members. A typical example of the moment-rotation curve for a joint in a structure excited by both horizontal and vertical ground motions is shown in Fig. 2. The single-bay frame contains a node at the center of the girder where half of the total girder mass is assumed concentrated. The nonlinearity of the response curve is the result of the vertical component of the ground motion acting on the mass at the center of the girder. It is apparent that the use of the yield moment rotation based on anti-symmetrical bending would only normalize the total nodal rotation. An adequate indication of the ductility requirement of the members would only be obtained if all members had the same end moment relationship.

The yield rotation for a typical member is a function of its yield moment, stiffness properties, and the moment conditions at the opposite end of the member. The general equation for the yield rotation can be written as $\theta_y = CM_pL/EI$, where C is the coefficient based on the moment condition at the opposite end of the member. Table 1 lists the value of C based on selected end moment conditions for the opposite end.

The coefficient C has a minimum value based on anti-symmetrical bending. Therefore, the use of the equation for θ_y based on anti-symmetrical bending will result in larger ductility and excursion ratio values for members not subjected to anti-symmetrical bending.

2. Ductility ratio based on curvature--The ductility ratio based on curvature (1, 2) is defined in terms of Fig. 3 as follows:

$$\mu_2 = \frac{\phi_{max}}{\phi_y} = \frac{\phi_y + \phi_o}{\phi_y} = 1 + \frac{\phi_o}{\phi_y} \tag{4}$$

where ϕ_{max} = maximum curvature, ϕ_y = curvature at yield, and ϕ_o = plastic curvature. For members which contain anti-symmetrical bending this equation for μ_2 is the same as for μ_1.

For bilinear systems this ratio can be expressed in terms of the moment value of Fig. 3 as follows:

$$\mu_2 = 1 + \frac{M_{max} - M_p}{pM_p} \tag{5}$$

where M_{max} = maximum moment at the end of a member, M_p = plastic moment of the member, and p = rate of strain hardening.

The excursion ratio ε_2 corresponding to the ductility ratio based on curvature can be defined as

$$\varepsilon_2 = \sum_{i=1}^{N_\mu} \frac{\phi_o}{\phi_y} = \sum_{i=1}^{N_\mu} (\mu_{2i} - 1) \tag{6}$$

where N_μ = total number of time the node of a member becomes plastic, and μ_{2i} = ductility ratio for the half cycle plastic rotation i. The excursion ratio can also be expressed in terms of bending moment or ductility ratio as:

$$\varepsilon_2 = \sum_{i=1}^{N_\mu} \frac{(M_{max})_i - M_p}{pM_p} = \sum_{i=1}^{N_\mu} (\mu_{2i} - 1) \tag{7}$$

Discussion of the method--A couple of advantages of the second definition for ductility over the first can be noted. First, as mentioned above, the ductility requirements based on curvature are applicable to nonsymmetrically loaded members as well as ones loaded symmetrically. Also, when analyzing bilinear systems, both the ductility and excursion ratios using the second definition can be determined from calculated end-moments.

Disadvantages of the method may be revealed by considering the reversal of the stress field occurring in flexural members. When a member has a stress reversal, the Bauschinger effect is present. This consists of the effect of straining a material in tension beyond its yield point and then reversing the load to obtain a lower yield point in compression than would be obtained if not initially placed in tension. This reduction is the result of residual stresses left in the material due to the tensile deformations. The Bauschinger effect is applicable to flexural members due to the stress reversals present above and below the neutral axis of the member cross-section.

There are several methods one can use to take into consideration the Bauschinger effect. The method used here and by most investigators consists of limiting the stress range or the elastic unloading range to $2M_p$. This causes the total elastic range of the material to remain constant. Figure 4 illustrates this method as applied to bilinear systems. A constant $2M_p$ is present in elasto-plastic systems by virtue of no strain hardening.

There are some questions as to the adaptability of the first two definitions of the ductility ratio when the stress range of $2M_p$ is used for bilinear systems. Figure 4 illustrates a situation which may

result in a misleading ductility ratio. In this situation the first bilinear half cycle of rotation results in a large amount of plastic rotation. With a $2M_p$ stress range, the second half cycle of rotation will have a low absolute magnitude for M_p; a corresponding low value for θ_y will result. Even though the amount of plastic rotation during the second half cycle of rotation is less than the first, a larger ductility ratio will result in misleading values for both half cycles of rotation.

3. Ductility ratio based on variable energy--The third definition for the ductility ratio is proposed herein which is intended for all member end conditions and loading conditions (2). The ductility ratio should reflect the maximum necessary plastic rotation which a member must withstand as related to its yield condition. The yield condition is a function of the end condition of the member at the time of the plastic rotation.

When plastic rotation of the end of a member occurs, energy is dissipated in the form of strain energy. For an elasto-plastic system the amount of strain energy dissipated during the plastic rotation is directly proportional to the amount of rotation. This relationship between plastic rotation and dissipated strain energy provides ways of formulating the ductility ratio based on dissipated strain energy. This third definition of ductility ratio can be stated as the ratio of the dissipated strain energy of a member end to the total elastic strain energy in the member plus one as

$$\mu_3 = 1 + \frac{E_{ds}}{E_{tes}} \tag{8}$$

where E_{ds} = dissipated strain energy of a member end during half cycle of joint rotation as shown in Fig. 5, and E_{tes} = total elastic strain energy in the member under consideration.

The excursion ratio based on the third definition for the ductility ratio is given below which indicates the total amount of energy that is dissipated in a node of a member due to plastic rotation:

$$\varepsilon_3 = \sum_{j=1}^{N_\mu} \frac{E_{dsj}}{E_{tesj}} = \sum_{j=1}^{N_\mu} (\mu_{3j} - 1) \tag{9}$$

where N_μ = total number of times joint becomes plastic during earthquake excitation, μ_{3j} = ductility ratio during half cycle j, E_{dsj} = dissipated strain energy during half cycle j, and E_{tesj} = total elastic strain energy in member while end-moment is maximum during half cycle j.

Discussion of the method--This third definition is similar to the previous definitions in that the ductility ratio is greater than one when plastic rotation occurs. Also, since the dissipated strain energy is related to the plastic rotation, any increase in the plastic rotation results in an increase in the dissipated strain energy and a corresponding increase in the ductility ratio. The total elastic strain

energy in a member is a function of the work produced by the end moments going through the end rotations while in the elastic range. The elastic strain energy of the total member is used so that the yield condition of the member end in question is based on the end conditions of both ends of the member. The elastic strain energy stored in a member by its end moments is independent of the manner in which the end moments are reached. Therefore, the above definition of ductility ratio is especially applicable to structures excited by both horizontal and vertical earthquake components where a nonlinear relationship of end-moment and rotation is present.

The maximum deviation a moment-rotation can have from the usual linear relationship is shown in Fig. 6 for an elasto-plastic system. Parallelogram ABCD establishes the boundary to be discussed. Lines OA and OB illustrate the linear paths for a member under anti-symmetrical bending and pure bending, respectively. Lines OC and OD correspond to the negative paths of the same two bending conditions. Curve OG represents a typical curve comparable to the curve in Fig. 2 where the moment-rotation relationship is nonlinear.

An example will be shown to illustrate that the elastic strain energy in a member is independent of the manner in which the final end moments are obtained. Assume the final bending condition of a beam consists of anti-symmetrical bending with an end moment of M_p as indicated by point A of Fig. 6. This condition is assumed to be reached by two different ways. First, let the member bending condition be reached by anti-symmetrical bending from the unloaded to loaded condition. The moment-rotation curve for each end of the member for this way of loading will be path OA of Fig. 6. Second, the moment at the right end of the member is decreased to a negative M_p value while no moment is applied to the left end; a rotation of $-M_pL/3EI$ and $-M_pL/6EI$ will result at the right and left ends of the member, respectively. Now with the simultaneous application of increasing moments of M_p and $2M_p$ to the left and right ends of the member, respectively, the final anti-symmetrical bending case is realized. The moment-rotation paths are also shown in Fig. 6. Dashed line OEA represents the left end while dashed line OHA represents the right end of the member.

The resulting elastic strain energy for each of the ways of increasing to the final anti-symmetrical bending is found from the area under the moment-rotation curves. These areas are shown in Fig. 7 for the second approach to the anti-symmetrical bending condition.

(1) Anti-symmetrical increase in end moments

$$E_{es1} = 2[\frac{1}{2}(\frac{M_p L}{6EI})]M_p = \frac{M_p^2 L}{6EI}$$

(2) Various increases in end moments

$$E_{es2} = 0 + \frac{1}{2}(\frac{-M_p L}{3EI})(-M_p) + \frac{1}{2}(\frac{M_p L}{4EI})(-M_p) + \frac{1}{2}(\frac{M_p L}{4EI})(M_p)$$

$$= \frac{M_p^2 L}{6EI}$$

Therefore, $E_{es1} = E_{es2}$, which illustrates that the elastic strain energy in a member is independent of the manner in which the final end moments are obtained. Apparently, the nonlinearity of the moment-rotation curves, when considering both horizontal and vertical earthquake components in conjunction with girder nodes, does not invalidate the third definition of the ductility ratio.

The advantages of the third definition for ductility ratio based on energy can be stated as follows:

1. Definition is general and applies to nonsymmetrical bending.
2. Definition is independent of the moment-curvature relationship assumed. Elasto-plastic, bilinear as well as the Ramberg-Osgood relationships can be used.
3. Definition is more adaptable when considering a bilinear response with a $2M_p$ elastic stress range.
4. No problem results when moment-rotation relationship is nonlinear due to inclusion of the vertical earthquake motion.
5. Dissipated and elastic energy values used in definition are easily determined from the area under the M-θ curve for the step-by-step method of analysis.
6. Definition is proportional to the energy dissipated in a node of a member due to plastic rotation.

The disadvantages to the third definition of the ductility ratio are that the actual nodal rotation in the plastic range cannot be found directly from the ductility ratio and that the ductility ratio may be overestimated when E_{tes} is relatively small during one of the cycling responses.

4. Ductility ratio based on mixed energy--This definition is similar to the third one except that the elastic strain energy of a member, E_{tes}; will be based on the plastic moments and the corresponding plastic rotations of the member (3). Thus E_{tes} is a constant as $M_p^2 L/6EI$. However, the dissipated strain energy will be the same as given in the previous definition. It is apparent that the pitfall of a small value of E_{tes} during any hysteresis loop, as discussed in variable energy, will not appear in this definition.

NUMERICAL EXAMPLES

Example 1--The ten-story, one-bay rigid frame shown in Fig. 8 is analyzed for the vertical and the N-S horizontal components of 1940 El Centro earthquakes. No magnification factor is included in the loading. Reduction of the allowable bending moment M_p in each column is

considered on the basis of the AISC specifications (4). The P-delta effect due to vertical dead load and ground motion is included in the analysis. Initial moments in the structure due to static loads are not included. The maximum ductility and excursion ratios for each girder of the elasto-plastic system are shown in Figs. 9 and 10 for each definition of ductility considered. Since the structure has strong columns, the plastic hinges only occur in the columns at the supports; consequently, the ductility and excursion ratios are not shown. The effect of interacting ground motions of each of the structural models on the ductility factor and excursion ratio are shown in Fig. 11. Figure 12 reveals the influence of damping on the ductility requirements.

Observations--The results shown in Figs. 9-12 may be summarized as follows:

1. A similar pattern in the variation of the girder ductility ratios based on the three definitions is realized for the structures studied. A qualitative determination of the ductility requirements could be made by either of the three definitions.

2. The ductility ratio based on symmetrical bending always yields a higher ratio than that obtained on the basis of curvature and energy. The ductility ratio based on energy seems higher than that defined by curvature.

3. Due to the lower value of the ductility ratios for the strong column frame, the difference in the ductility definitions are not as significant as in the structures with weak columns which are not included in the paper.

4. The use of the ductility ratio based on energy provides a reasonable estimator of the ductility requirement of a structure containing members having unsymmetrical bending and a constant stress range.

5. Model 2 provides a better simulation of a structural system by allowing possible plastic hinges to occur at the center of girders.

6. Vertical ground motion affects the response parameters more for Model 2 than Model 1 particularly on structures with weaker columns.

7. The maximum ductility requirements for the ten-story frame occur approximately at the quarter points in its height.

Example 2--The ten-story and one-bay three-dimensional building system shown in Fig. 13 has rigid concrete floors for which the columns have the deformations of torsional, axial, and bending about both major and minor axes of individual members. Because of the rigid slab, each floor should have two common translatory movements and one rotation. The formulation of the structural system may be found in Ref (3, 5).

The material behavior is given in Figs. 14 and 15 for which a = 1 and γ = 20 are used in this example. The moment-rotation relationships about both axes of column No. 3 at fifth floor are shown in Figs. 16 and 17 (top column) as well as 18 and 19 (bottom column). The results are due to two dimensional ground motions of N-S (applied in x-direction) and E-W (in y-direction) of El Centro 1940. The comparisons of ductility factors about the major axis of columns, resulting from N-S component, are given in Fig. 20; the comparisons of the ductility factors about the major axis influenced by the three components are shown in Fig. 21. In the example, the scale of the N-S and the vertical components in three; however, no scale is used for the E-W component because this one-bay structure is considerably weak in y-direction. All the analyses are based on the eight seconds of earthquake record and the P-Δ effect is considered but no damping is included.

Observations--This example reveals that the interacting ground motion can yield very complicated hystersis loops of moment-rotation relationships of a three-dimensional system. Apparently there is not a conclusive definition of ductility for exactly measuring the inelastic deformation of such a structure. However, the patterns of the ductility factors based on rotation, variable energy, and mixed energy are very similar. Also worthy to note that the one-dimensional ground motion demands larger ductility on the top floor while the three-dimensional interacting motions significantly influence the ductility factors at the eighth floor. The ductility factors based on rotations are always the largest. However, the definition based on the mixed energy yields the least, and is believed to be the most accurate one for the three-dimensional response analysis.

ACKNOWLEDGEMENTS

This paper is a partial work from the research project sponsored by the National Science Foundation, Grant No. NSF ENV75 18372 A01. This support is gratefully acknowledged.

REFERENCES

1. Cheng, F.Y. and Oster, K.B., Dynamic Instability and Ultimate Capacity of Inelastic Systems Parametrically Excited by Earthquakes--Part II, NSF Report, August, 1976, National Technical Information Service, Springfield, Va 22151, Access No. PB261097.

2. Mahin, S.A. and Berteo, V.V., "Problems in Establishing and Predicting Ductility in Aseismic Design", Proceedings of the International Symposium on Earthquake Structural Engineering, University of Missouri-Rolla, 1976, Volume I, pp. 613-628.

3. Cheng, F.Y. and Kitipitayangkul, P., Investigation of the Effect of 3-D Parametric Earthquake Motions on Inelastic Building Systems, NSF Report to be available in August 1979.

4. Manual of Steel Construction, 7th Edit. American Institute of Steel Construction, New York, N.Y.

5. Cheng, F.Y., "Comparatively Studies of Buckling Capacity of Three-Dimensional Building Systems", Proceedings of the International Colloquium on Stability of Structures under Static and Dynamic Loads, ASCE, 1977, pp. 179-193.

Table 1. Value of C in $\theta_y = CM_pL/EI$ Based on Different Conditions of Opposite End of a Member

Moment at Opposite End (clockwise positive)	Value of C
M_p	1/6
$M_p/2$	1/4
0	1/3
$-M_p/2$	5/12
$-M_p$	1/2

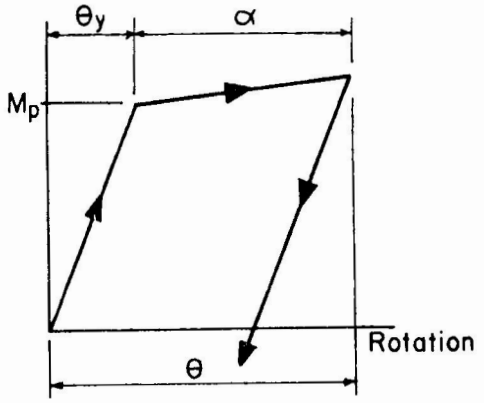

Fig. 1. Moment-Rotation, Ductility Based on Rotation

Fig. 2. M-θ Curve of Node 3 for Horizontal and Vertical Ground Motions of 1940 El Centro

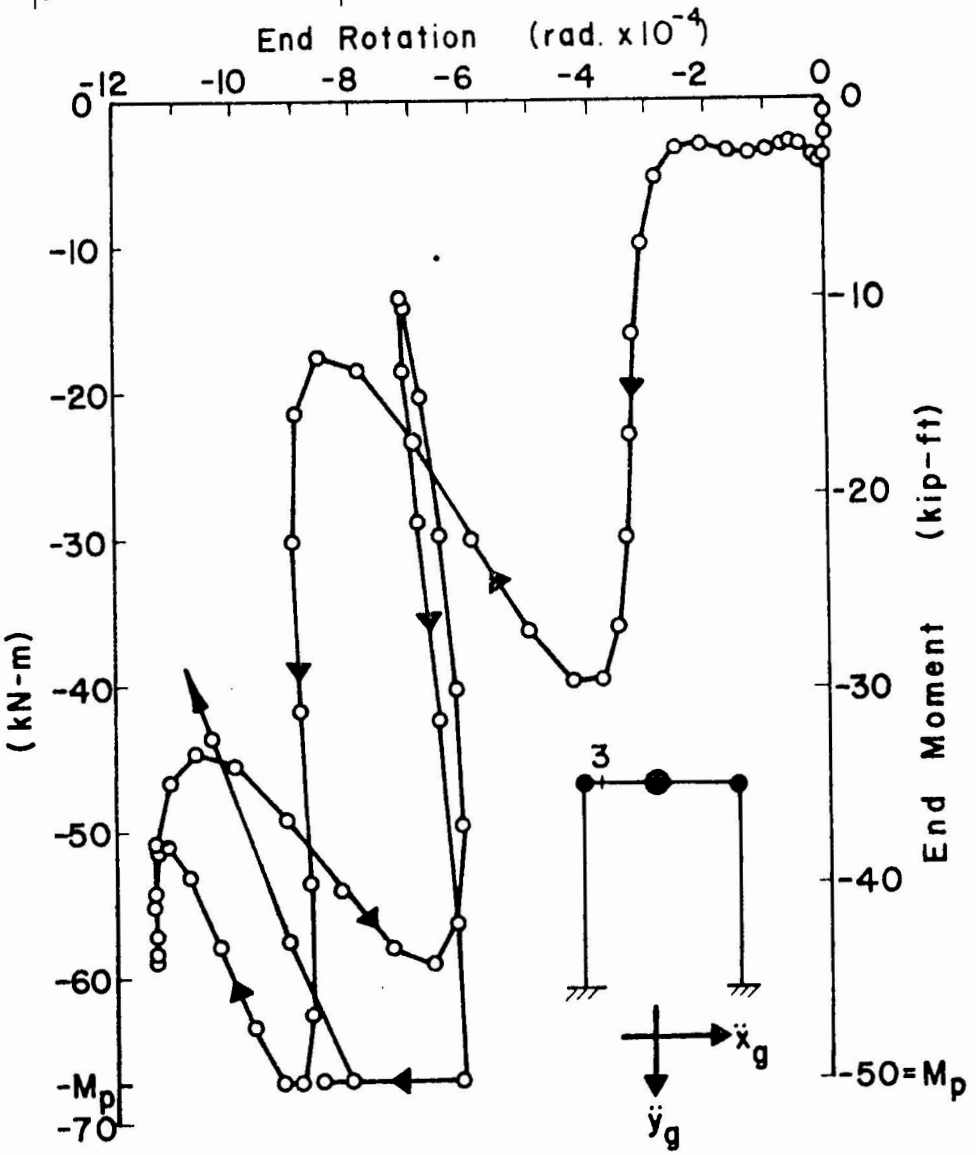

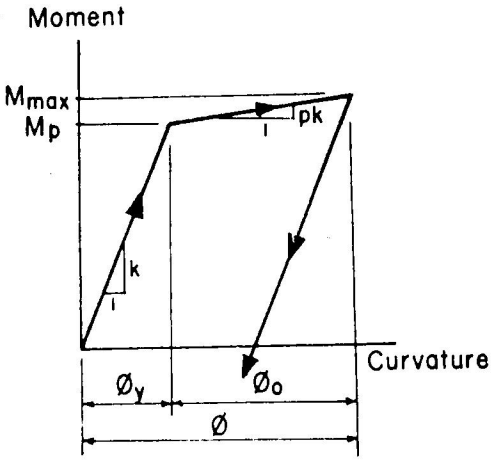

Fig. 3. Moment-Rotation, Ductility Based on Curvature

Fig. 4. Effect of $2M_p$ Stress Range on Ductility

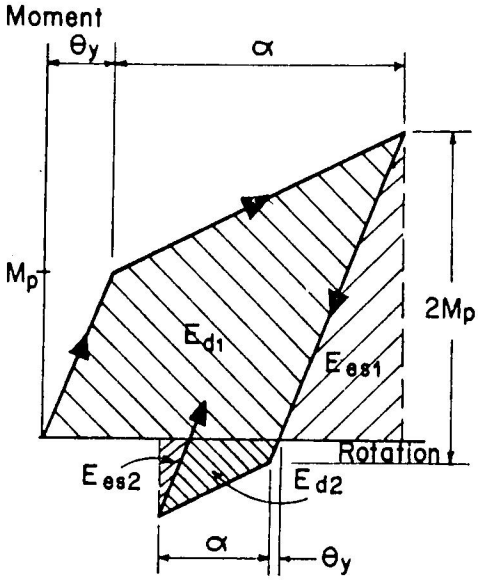

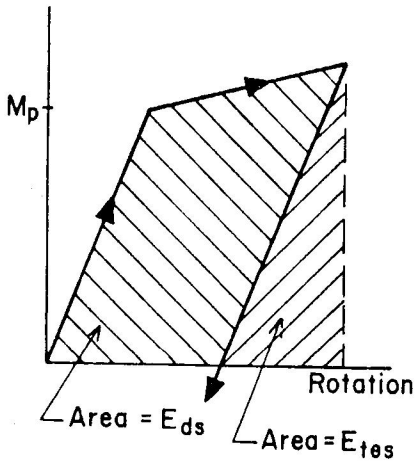

Fig. 5. Moment-Rotation, Ductility Based on Variable Energy

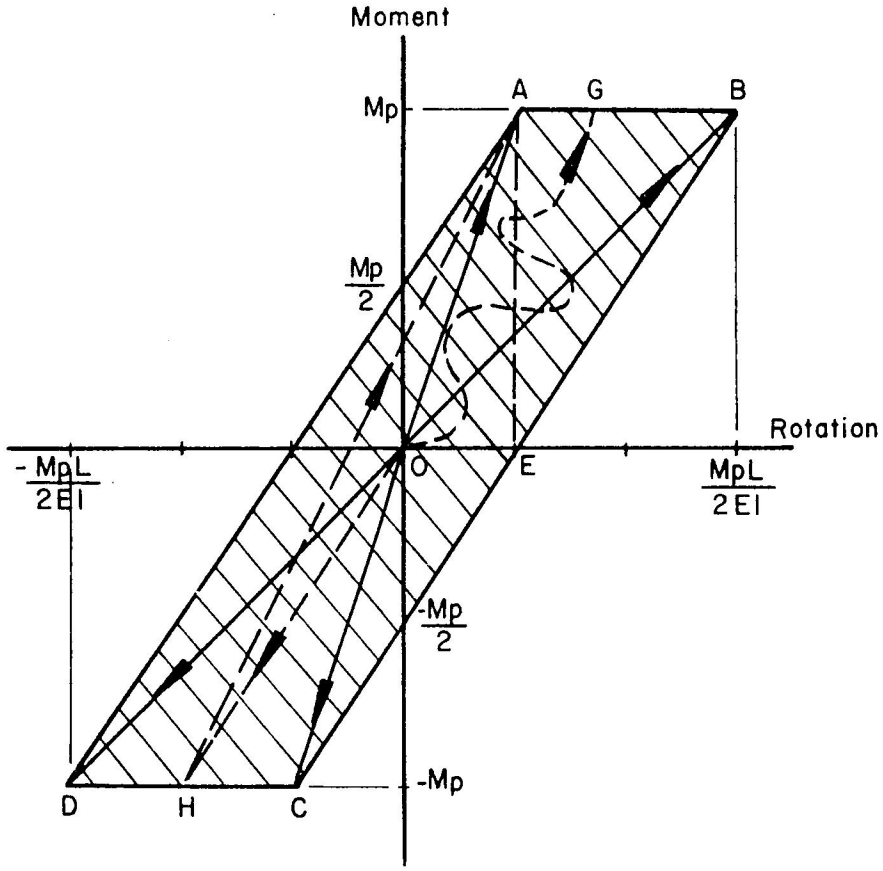

Fig. 6. Moment-Rotation Boundary for One End of a Member

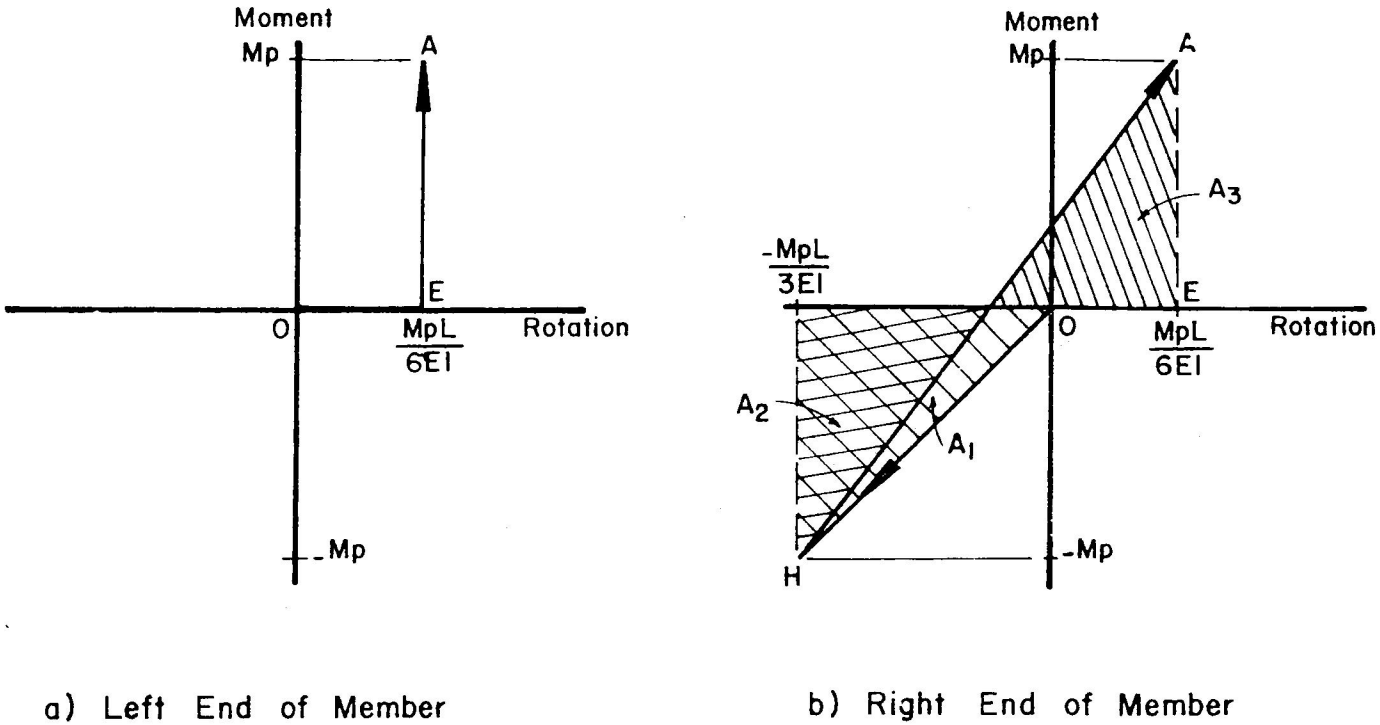

Fig. 7. Elastic Strain Energy of a Member Based on M-θ Relationship

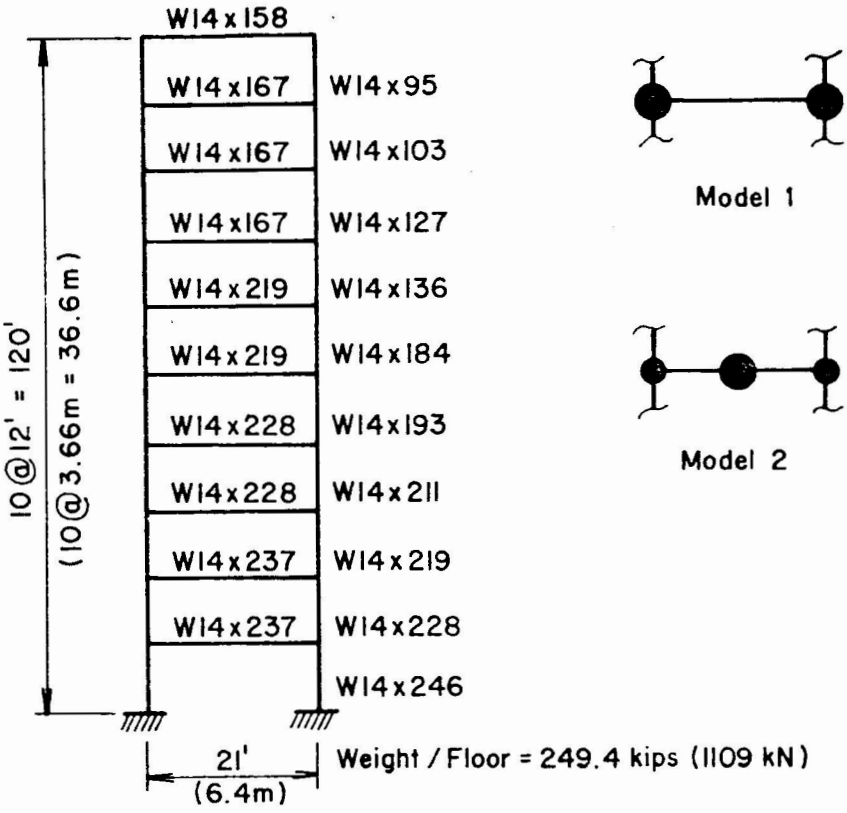

Fig. 8. 10-Story, 1-Bay Plane Frame of Example 1

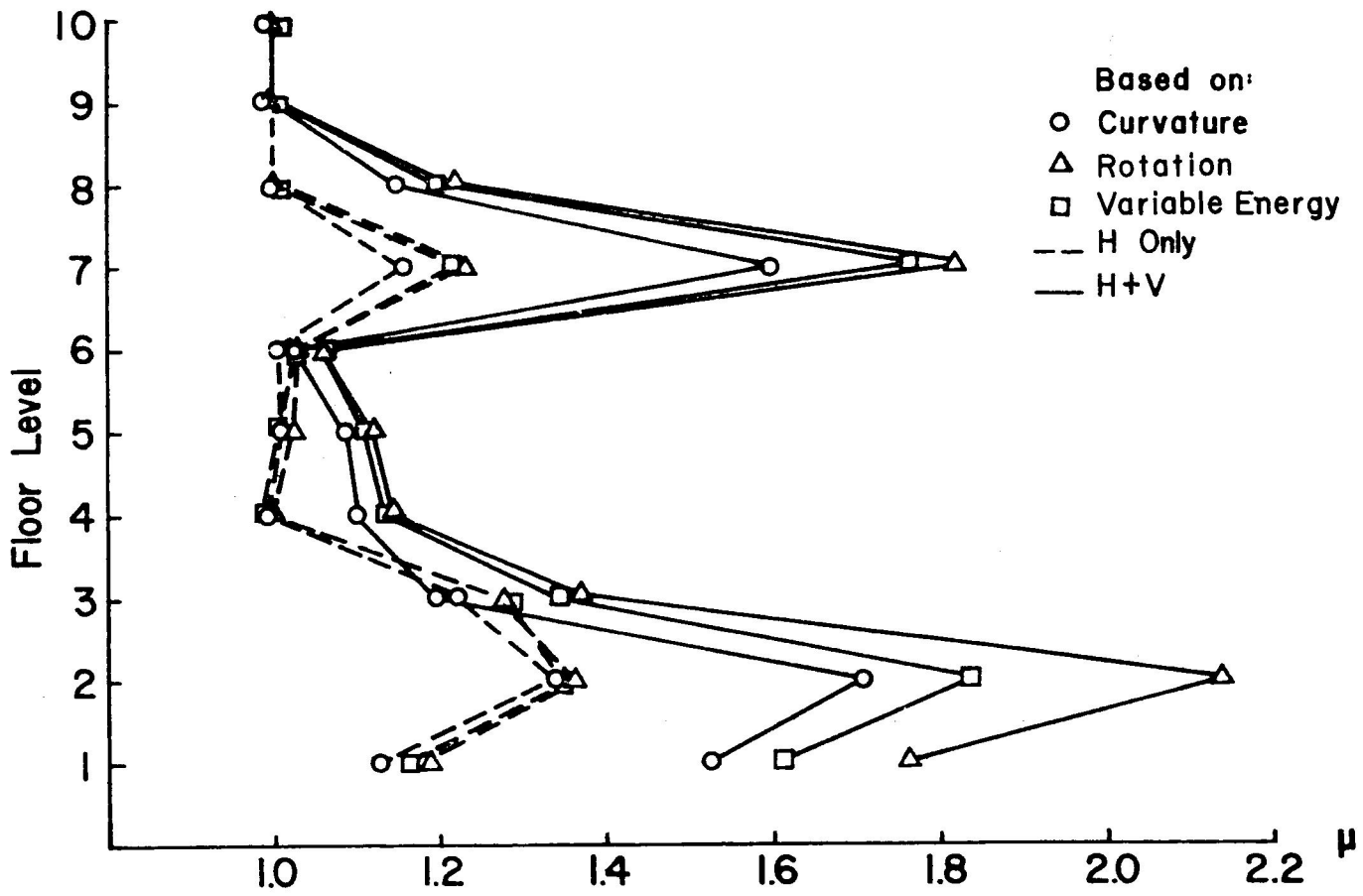

Fig. 9. Elasto-Plastic Girder Ductility Ratios of Fig. 9, 1940 El Centro

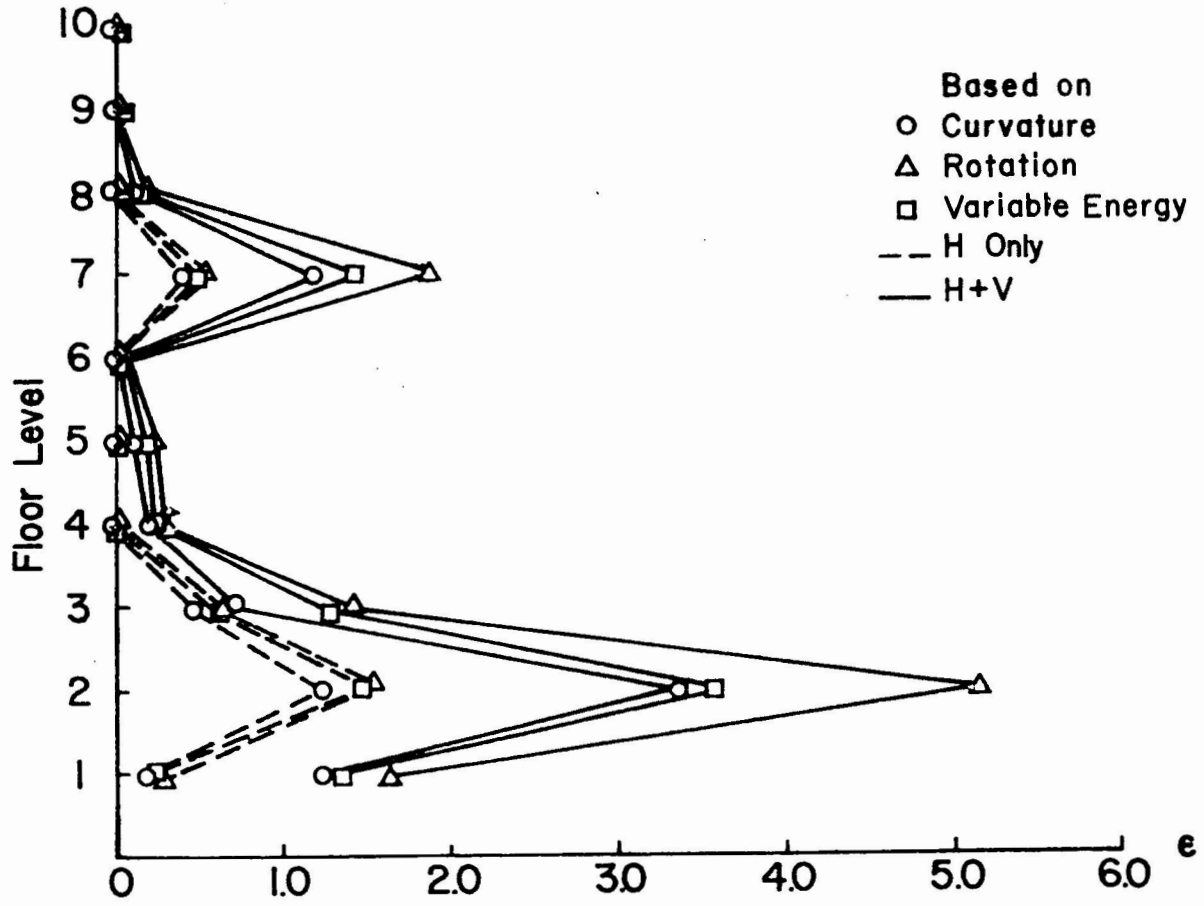

Fig. 10. Elasto-Plastic Girder Excursion Ratios of Fig. 9, 1940 El Centro

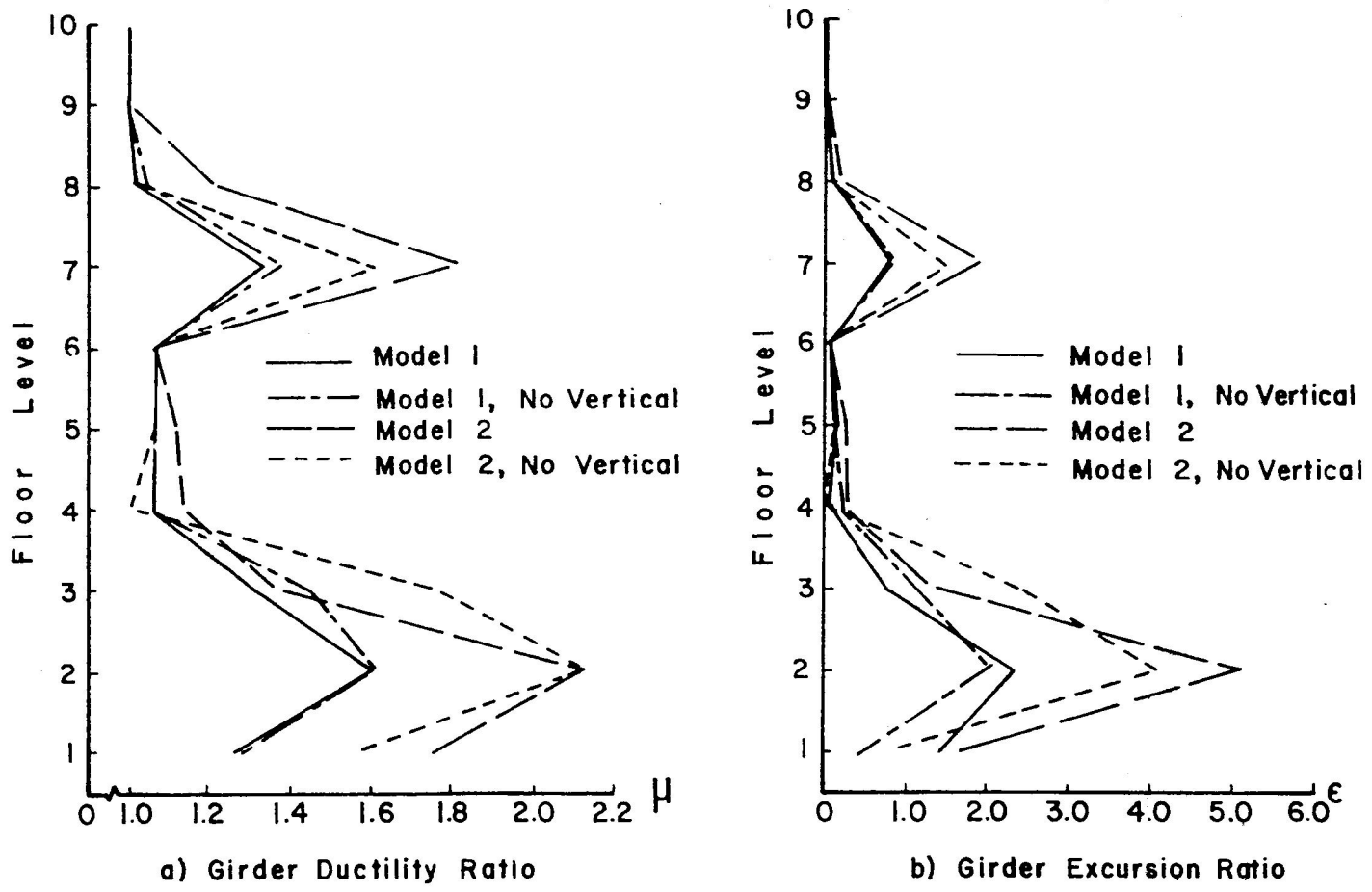

Fig. 11. Models 1 and 2 Ductility Requirement of Fig. 9, 1940 El Centro

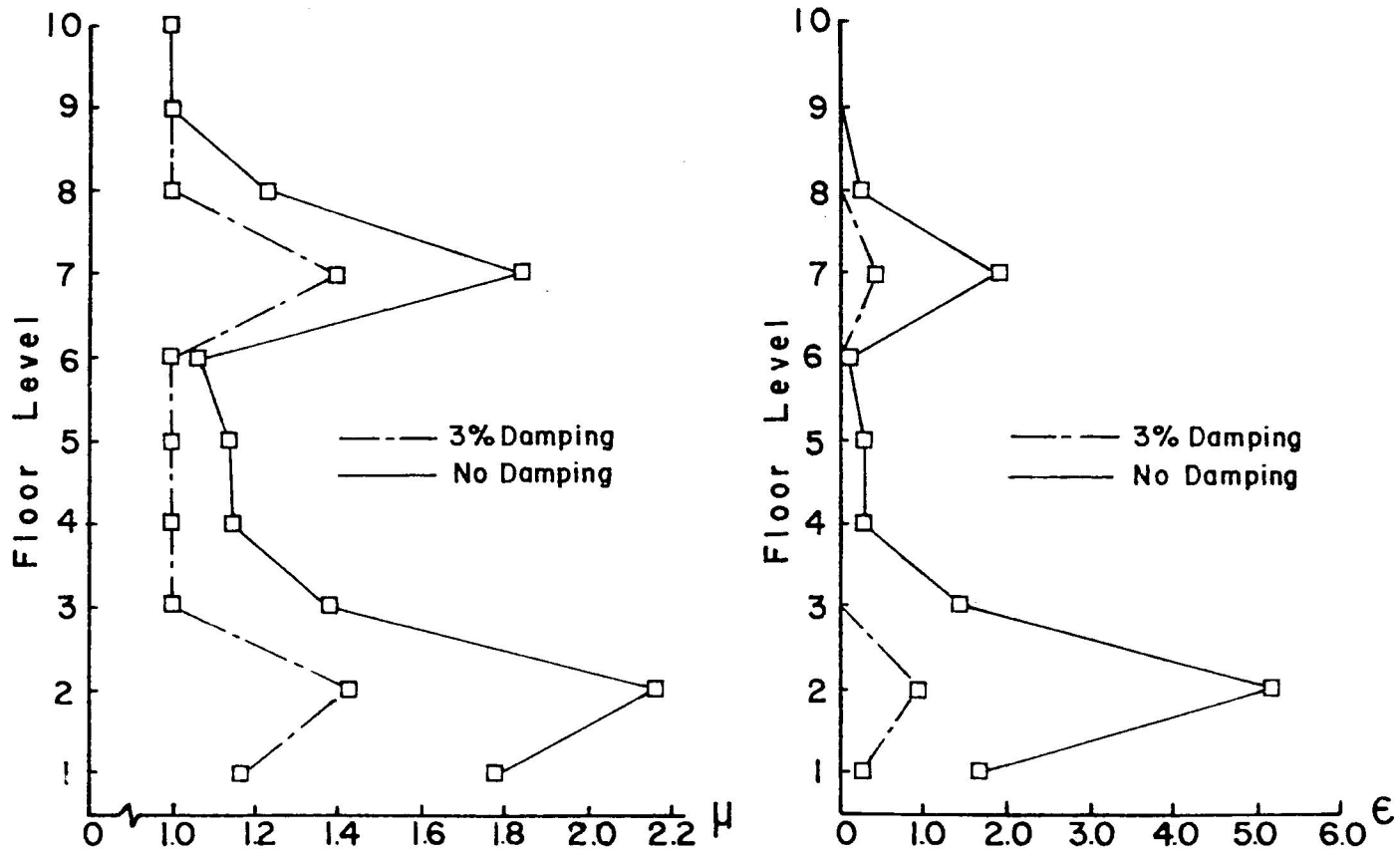

Fig. 12. Effect of Damping on Girder ductility Requirements, Elasto-Plastic System, 1940 El Centro, N-S Plus Vertical

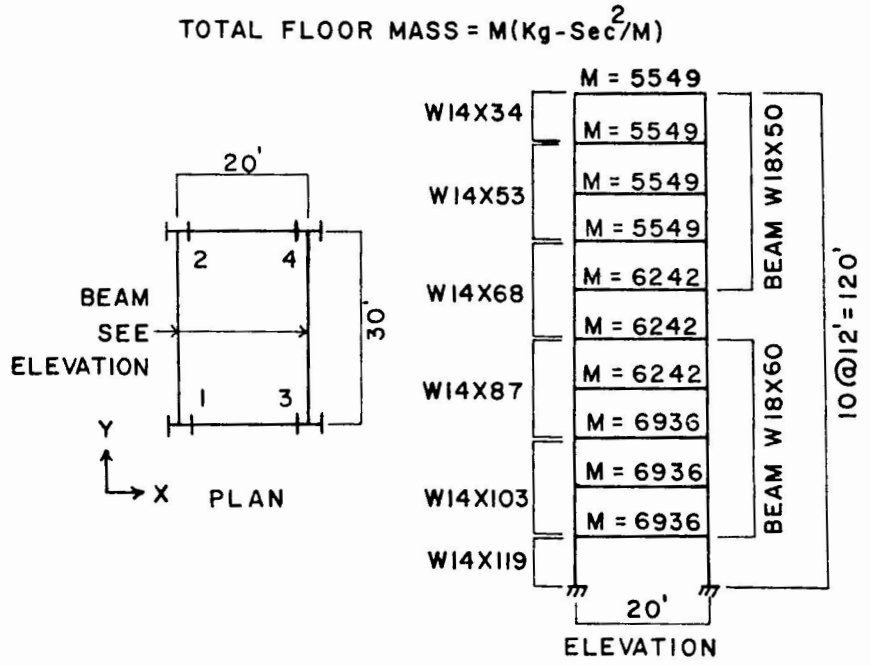

Fig. 13. 10-Story, 1-Bay 3-D Building System of Example 2

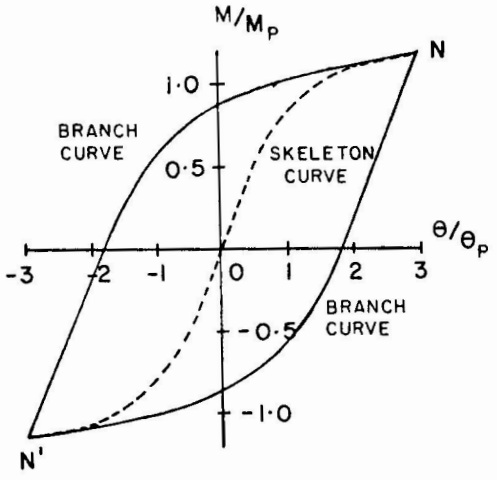

Fig. 14. Ramberg-Osgood Moment Reversal

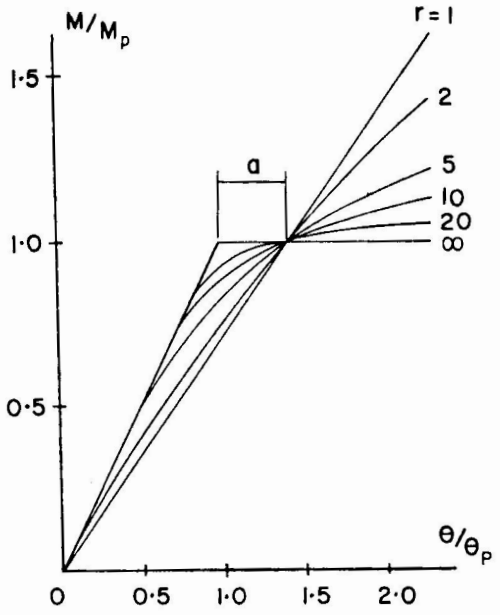

Fig. 15. Ramberg-Osgood M-θ For Secant Stiffness

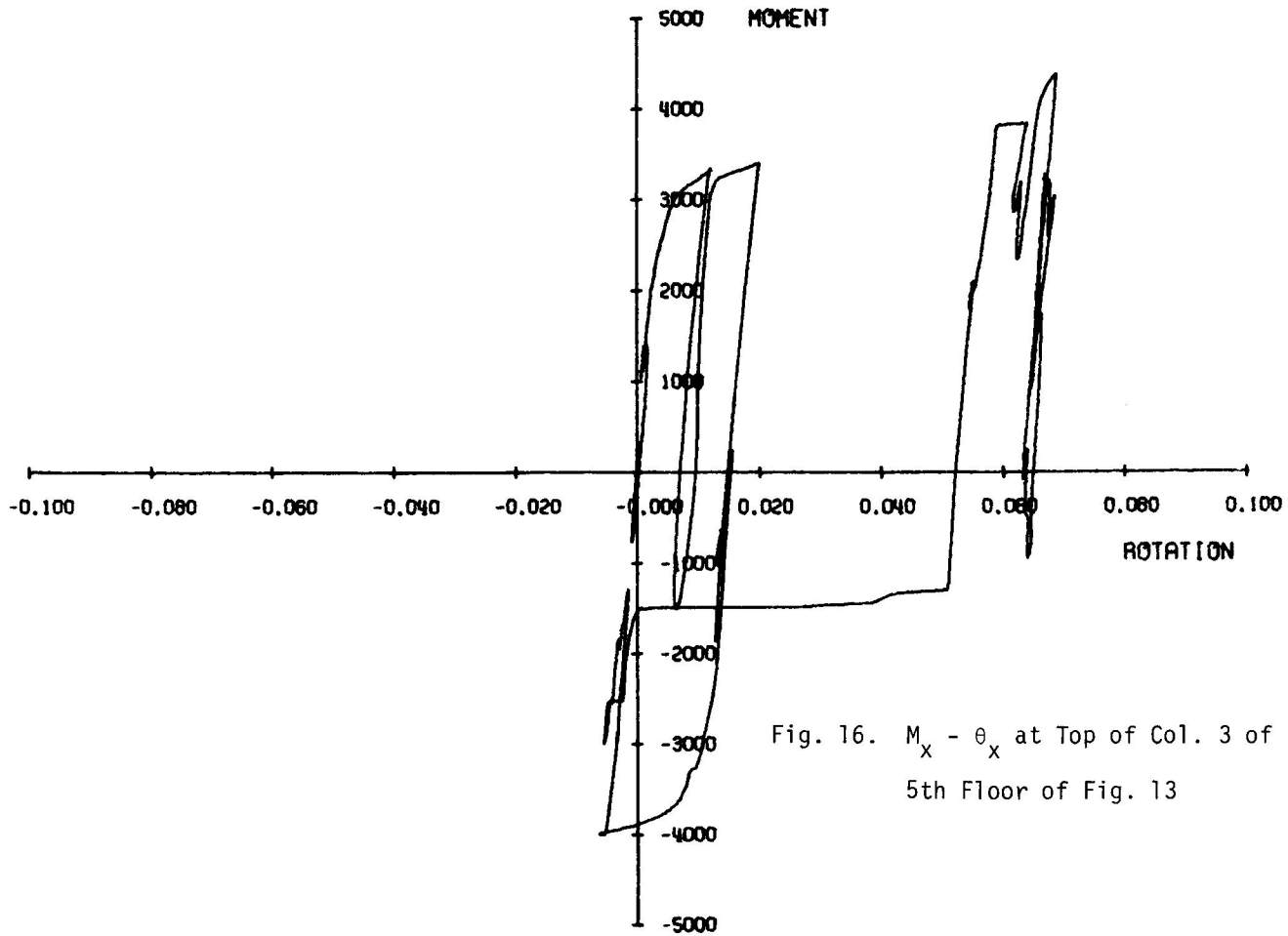

Fig. 16. $M_x - \theta_x$ at Top of Col. 3 of 5th Floor of Fig. 13

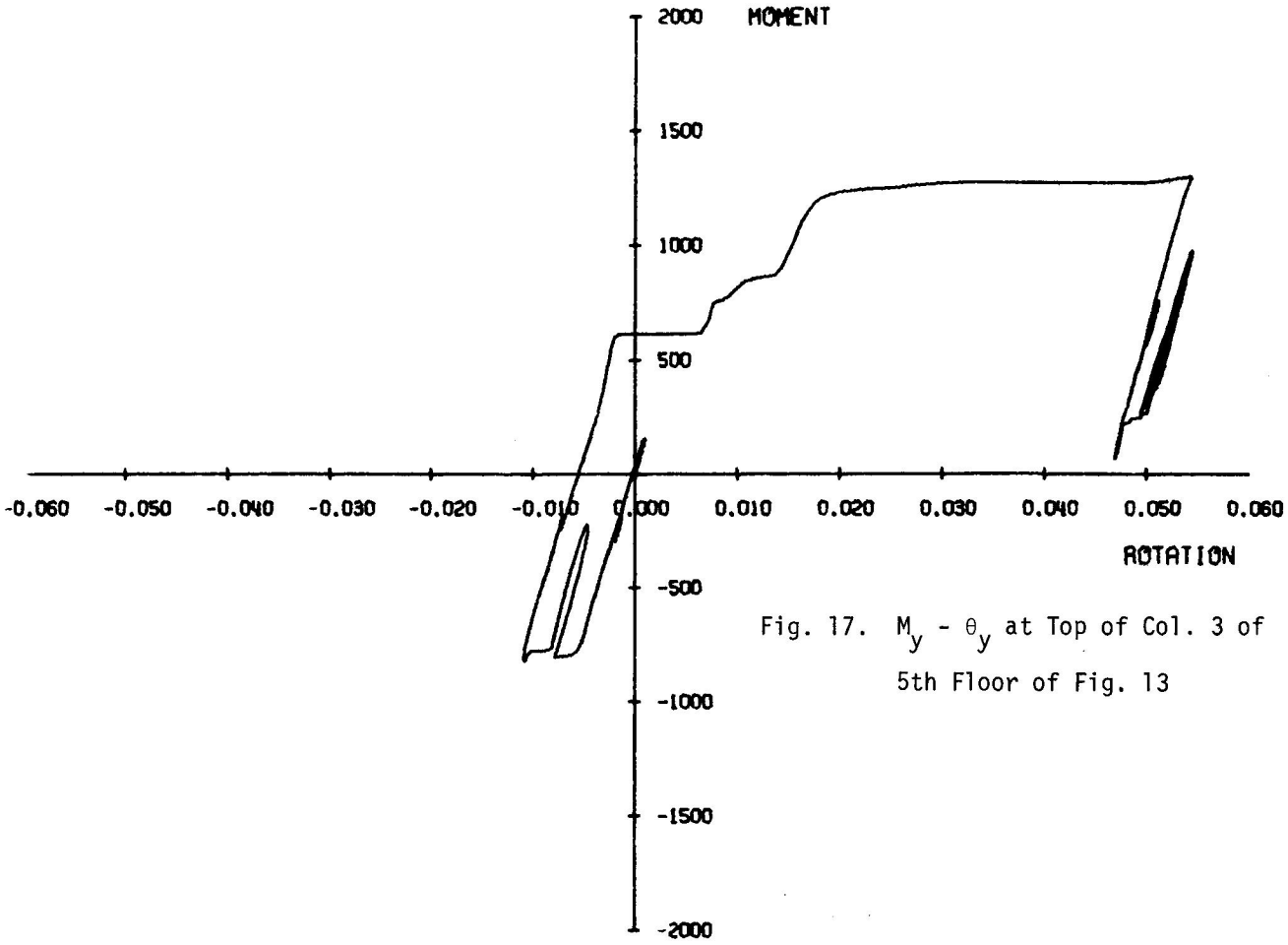

Fig. 17. $M_y - \theta_y$ at Top of Col. 3 of 5th Floor of Fig. 13

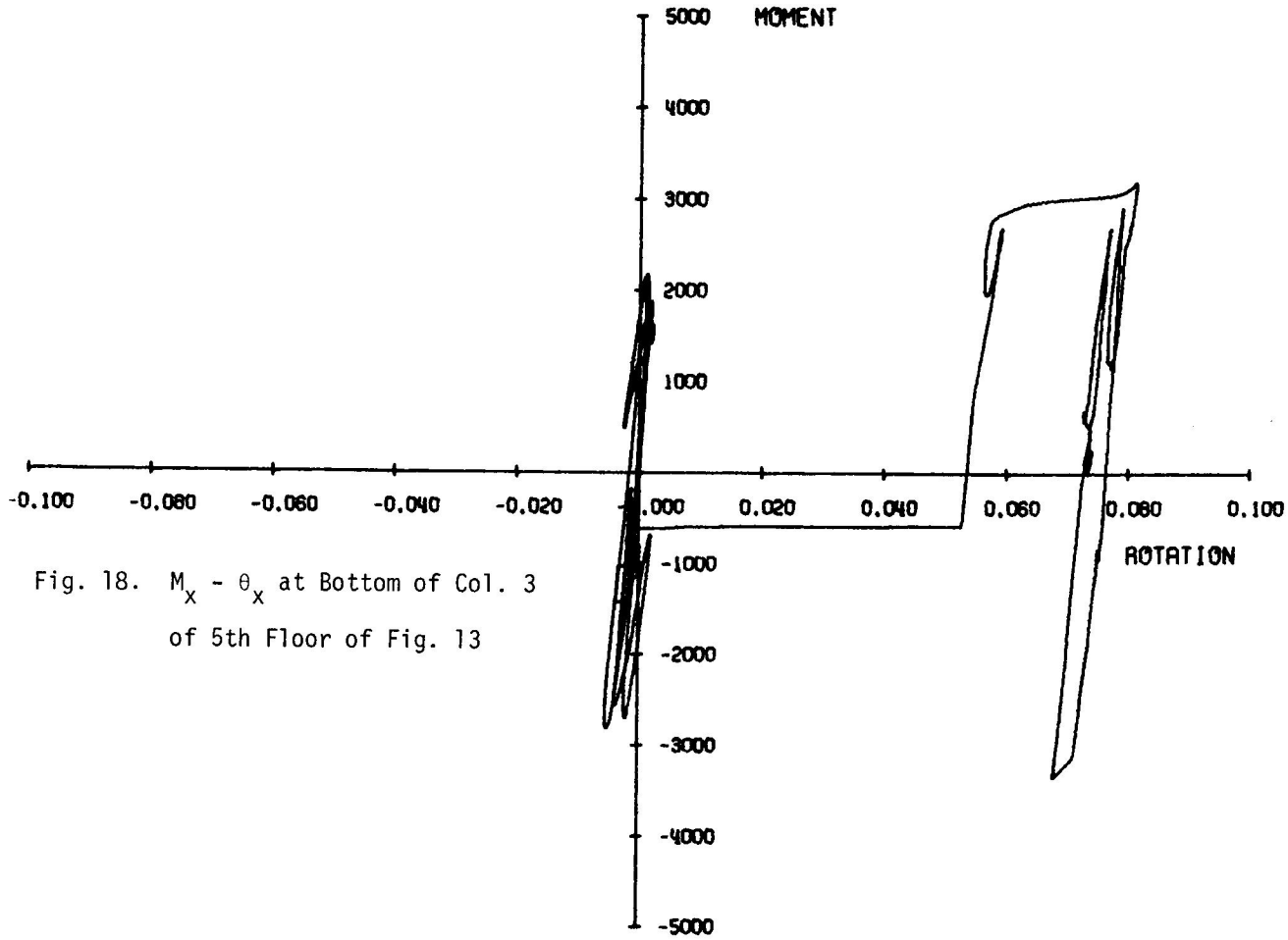

Fig. 18. $M_x - \theta_x$ at Bottom of Col. 3 of 5th Floor of Fig. 13

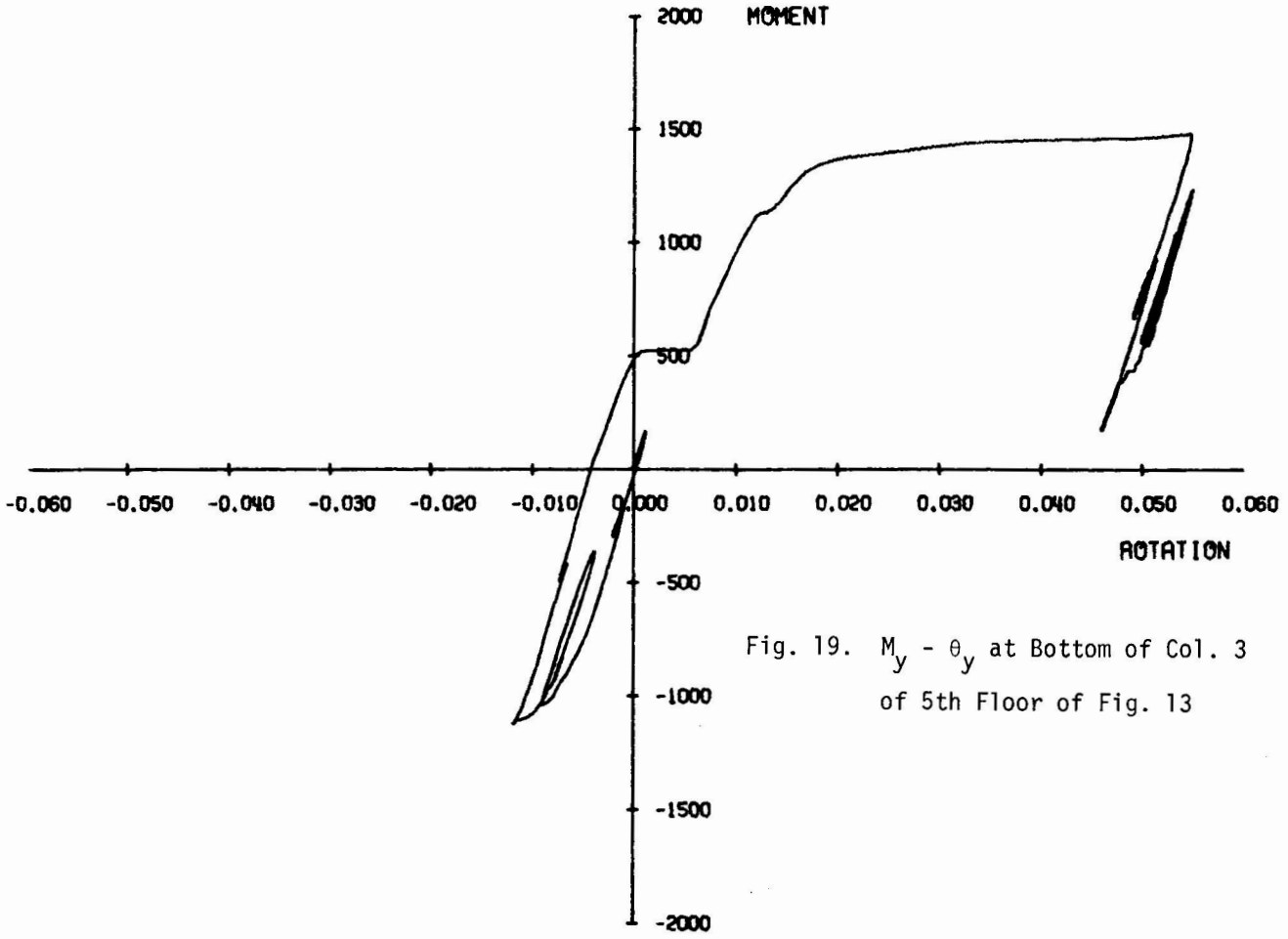

Fig. 19. $M_y - \theta_y$ at Bottom of Col. 3 of 5th Floor of Fig. 13

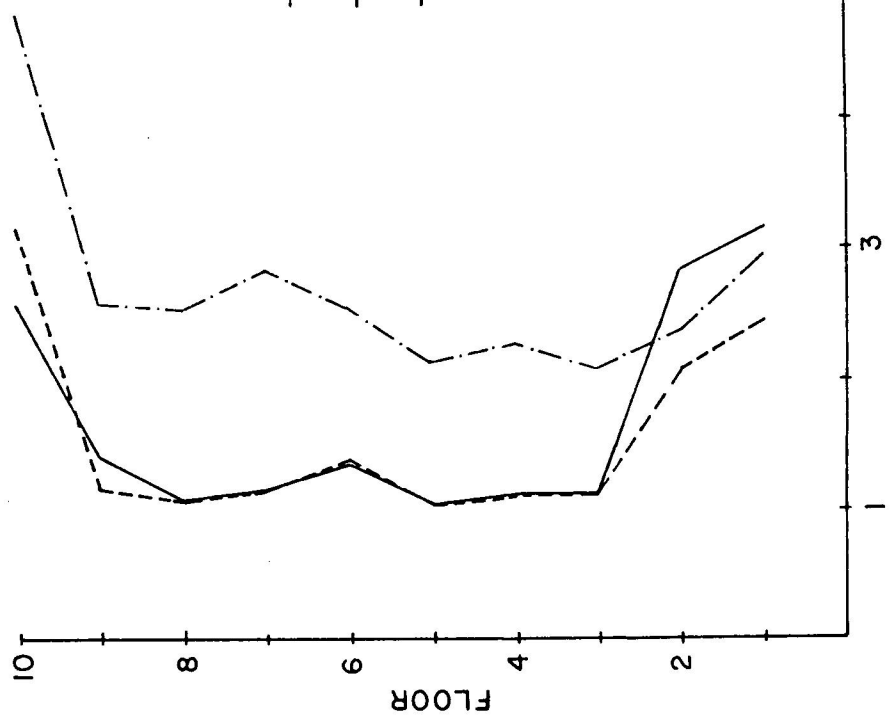

Fig. 20. Column Ductilities About X Axis of Fig. 13 for N-S Component of 1940 El Centro

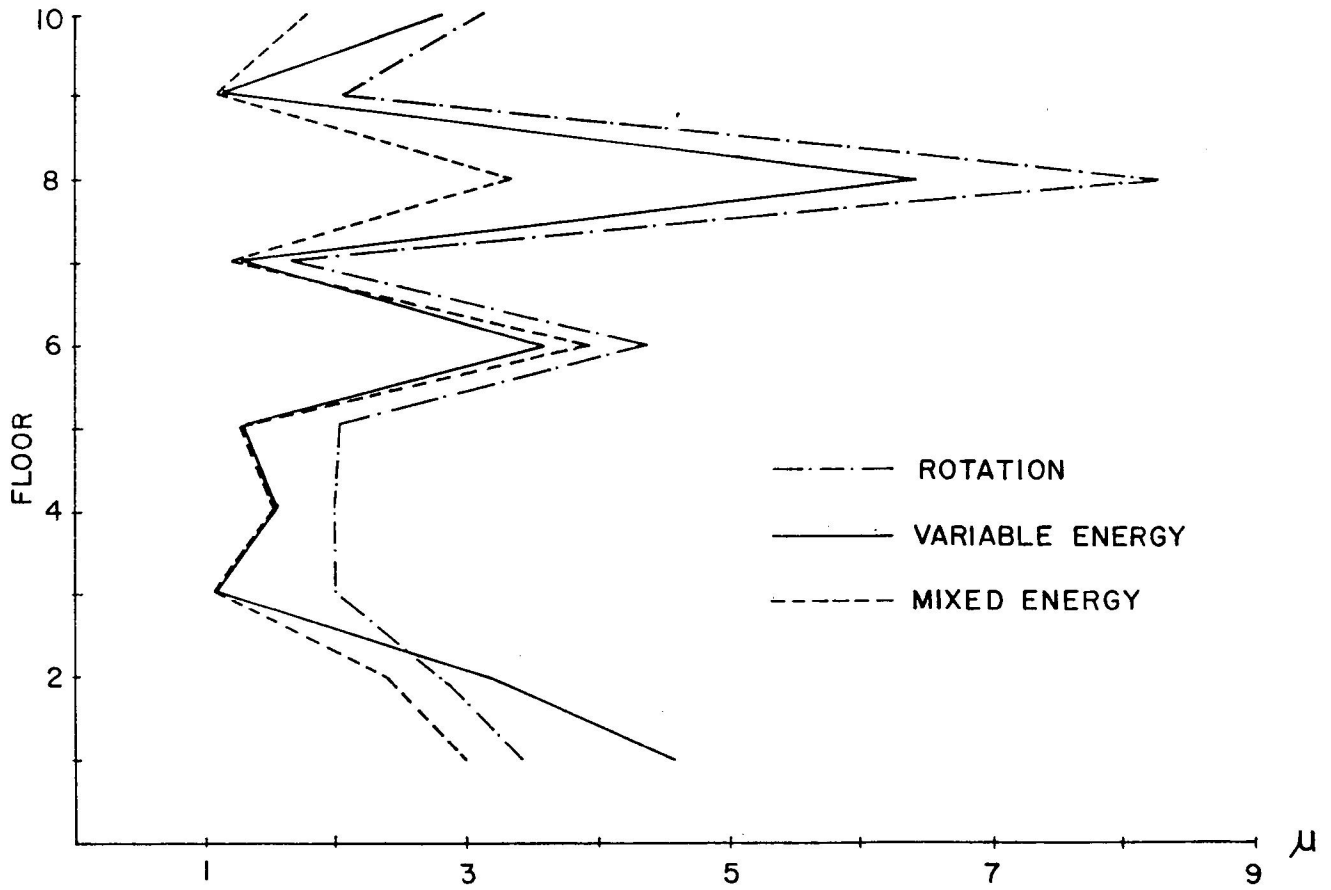

Fig. 21. Column Ductilities About X Axis of Fig. 13 for N-S, E-W, and Vertical Components of 1940 El Centro

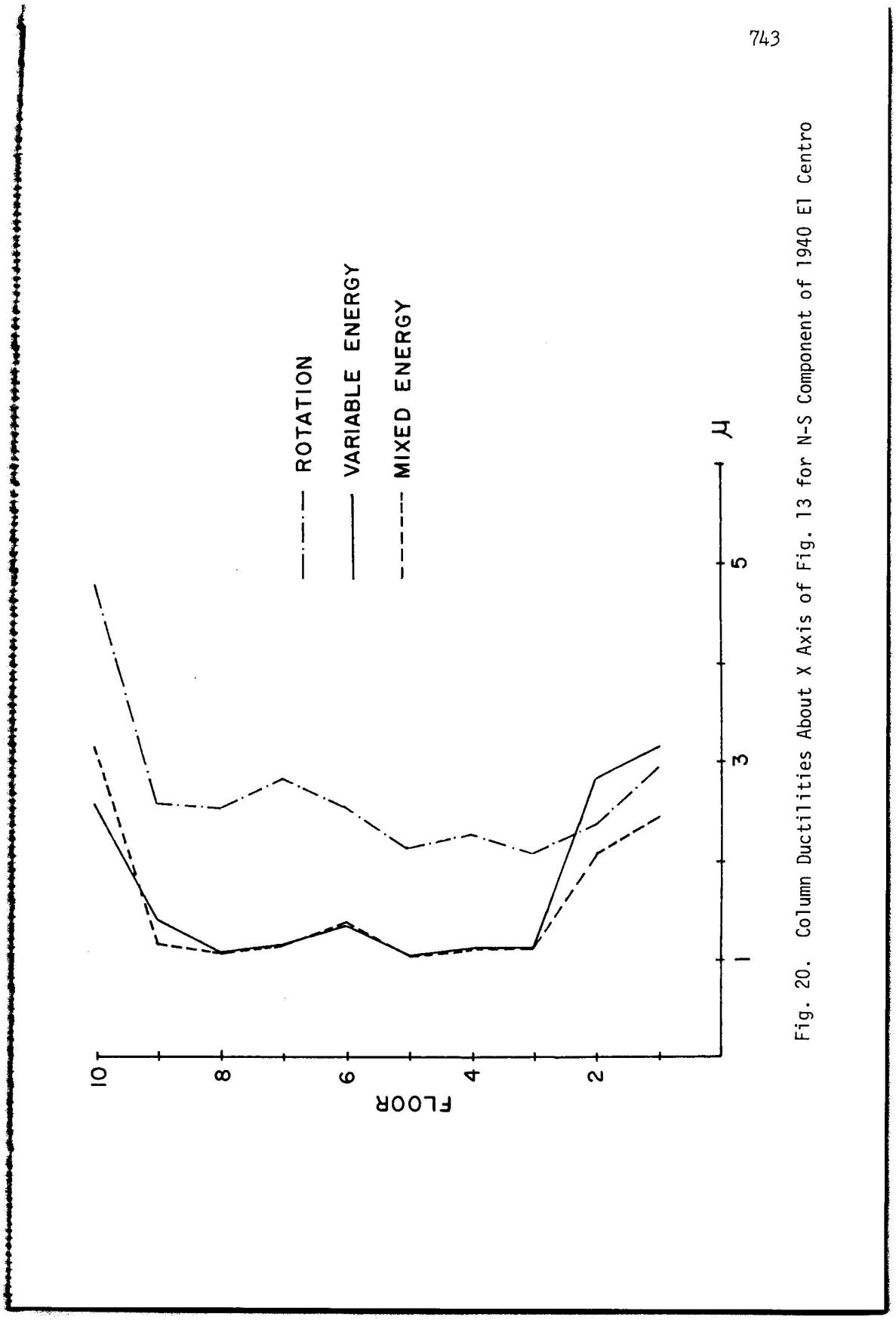

Fig. 20. Column Ductilities About X Axis of Fig. 13 for N-S Component of 1940 El Centro

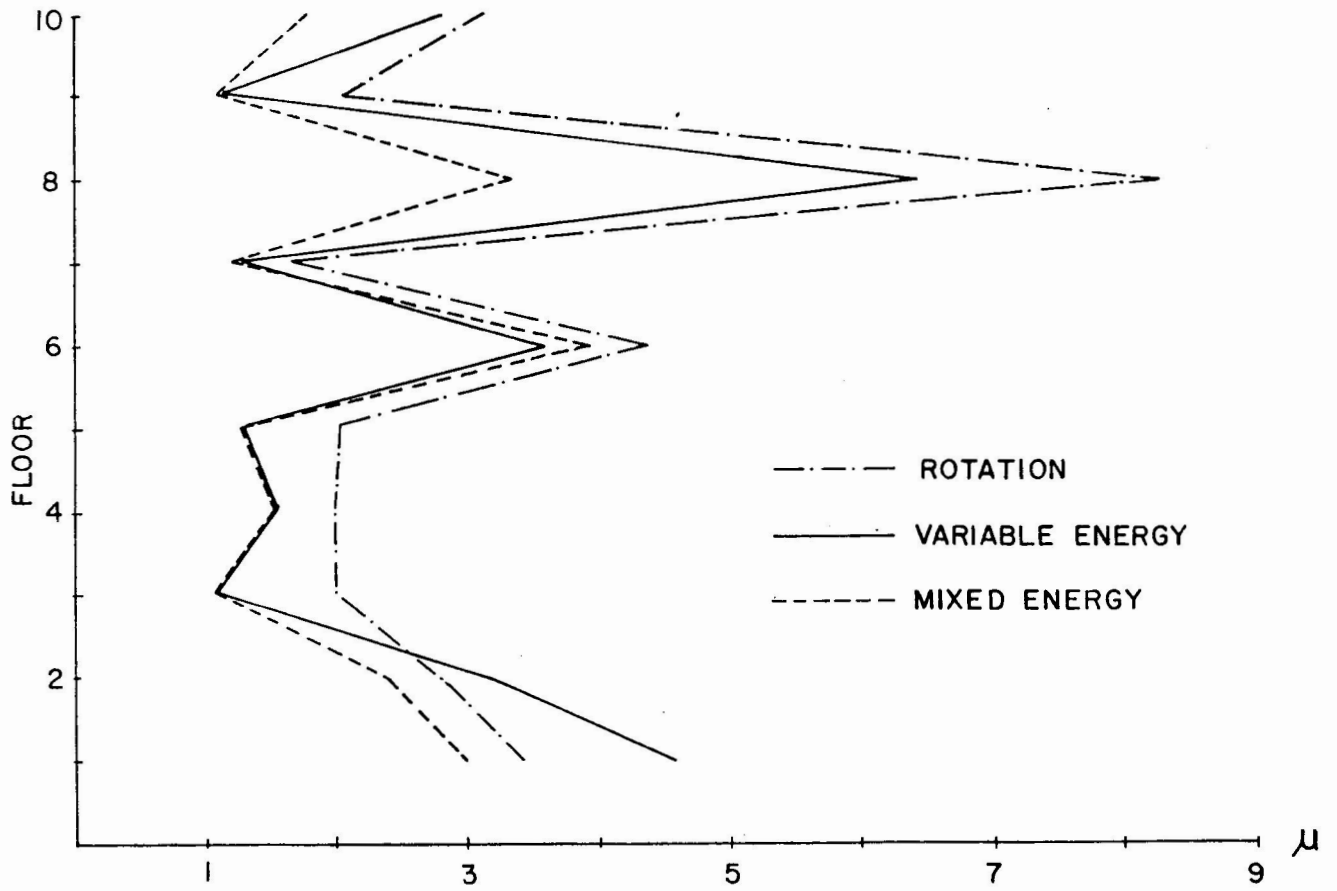

Fig. 21. Column Ductilities About X Axis of Fig. 13 for N-S, E-W, and Vertical Components of 1940 El Centro